Journal of Hydrology: Regional Studies 5 (2016) 309–323

Contents lists available at ScienceDirect

Journal of Hydrology: Regional Studies

journal homepage: www.elsevier.com/locate/ejrh

Regional climate change projections of streamflow characteristics in the Northeast and Midwest U.S.

Eleonora M.C. Demaria[a,*], Richard N. Palmer[a,b], Joshua K. Roundy[c]

[a] Northeast Climate Science Center, University of Massachusetts, 222 Marston Hall, Natural Resources Road, Amherst, MA 01003-9293, USA

[b] Department of Civil and Environmental Engineering, University of Massachusetts, 222 Marston Hall, Natural Resources Road, Amherst, MA 01003-9293, USA

[c] Department of Civil, Environmental, and Architectural Engineering, University of Kansas, 1530 W. 15th Street, 2150 Learned, Lawrence, KS 66045, USA

ARTICLE INFO

Article history:
Received 1 August 2015
Received in revised form 5 November 2015
Accepted 10 November 2015
Available online 8 December 2015

Keywords:
Streamflow peaks
Low flows
Trend analysis
Intense precipitation
Base flows

ABSTRACT

Study region: Northeast and Midwest, United States.
Study focus: Assessing the climate change impacts on the basin scale is important for water and natural resource managers. Here, the presence of monotonic trends and changes in climate-driven simulated 3-day peak flows, 7-day low flows, and mean base flows are evaluated in the Northeast and Midwest U.S. during the 20th and the 21st centuries using climate projections from sixteen climate models. Proven statistical methods are used to spatially and temporally disaggregate precipitation and temperature fields to a finer resolution before being used as drivers for a hydrological model.
New hydrological insights for the region: Changes in the annual cycle of precipitation are likely to occur during the 21st century as winter precipitation increases and warmer temperatures reduce snow coverage across the entire domain especially in the northern basins. Maximum precipitation intensities are projected to become more intense across the region by mid-century especially along the coast. Positive trends in 3-day peak flows are also projected in the region as a result of the more intense precipitation, whereas the magnitude of 7-day low flows and mean base flows are projected to decrease. The length of the low flows season will likely extend by mid-century despite the increased precipitation as the atmospheric demand increases.

1. Introduction

Changes in the magnitude and frequency of river flows can have significant impacts on freshwater resources for the ecosystem and human activities. Shifts in the volume and timing of streamflows can be critical to aquatic species that rely on them for important transitions in their life cycle, which can affect the existing infrastructure, and impact the water quality and the quantity for human water supply (Barnett et al., 2005; Comte et al., 2013; Hayhoe et al., 2007). The Northeast Climate Science Center (NE CSC) was established in 2012 by the Department of the Interior to address the regional challenges of climate variability and change in the Northeast and Midwest of the US. The NE CSC study area encompasses the 22 U.S.

* Corresponding author. Present address: Southwest Watershed Research Center, USDA-Agricultural Research Service, 2000 E. Allen Road Tucson, AZ 85719, USA.
E-mail address: eleonora.demaria@ars.usda.gov (E.M.C. Demaria).

http://dx.doi.org/10.1016/j.ejrh.2015.11.007

states east of the −98° W meridian and north of 36° N latitude. This region is inhabited by 131 million people (40% of the U.S. population), and the population is projected to increase by 20% by the year 2050 which will impose more stress on an already affected natural ecosystem and will have long-term impacts on the ecological and socioeconomic systems. This region contains several basins of economic and ecologic importance in the country, such as the Great Lakes Drainage, the Upper Mississippi river basin, the Ohio River basin, and the Connecticut River basin.

There is strong evidence that the intensity of precipitation events in the Northeast (NE) U.S. has increased in the 20th century as a result of anthropogenic effects in the hydrological cycle (Brown et al., 2010; Changnon, 2002; Douglas and Fairbank, 2011; Easterling et al., 2000; Groisman et al., 2001; Guilbert et al., 2015; Mishra and Lettenmaier, 2011). Heavy downpours, the events that are exceeded 1% of the time in any given year, have increased by 71% in the Northeast and 37% in the Midwest during the last three to five decades (Walsh et al., 2014). However, studies have found that the magnitude of annual maximum streamflows in the NE has not necessarily increased accordingly (Douglas et al., 2000; Lins and Slack, 1999, 2005; Villarini and Smith, 2010; Villarini et al., 2011). Positive trends in the number of high-frequency floods (5-year return period) have been found in most New England rivers throughout the 20th and early 21st centuries with a steep increase around 1970 (Armstrong et al., 2012). More frequent extreme streamflow events (above the 95th percentile) have been observed in the 21st century during the warm season in New England (Frei et al., 2015). In addition, earlier winter-spring flows in the range of 6–8 days has also been observed in the region and is thought to be linked to increased snow melting and rain-on-snow episodes (Hodgkins and Dudley, 2006), and this trend is likely to continue during the 21st century (Campbell et al., 2011). Increases in the magnitude and frequency of flood events have been observed in the central United States during the period of 1962–2011 (Mallakpour and Villarini, 2015).

Mean annual flows have increased in the eastern part of the United States during the last half of the 20th century (Collins, 2009; Hodgkins et al., 2005; McCabe and Wolock, 2011). Furthermore, low flows or base flows (groundwater contribution) have also shown robust upward trends (Douglas et al., 2000; Lins and Slack, 2005) that have been linked to the increasing precipitation during the summer in New England (Hodgkins et al., 2005), and during the fall in the upper Mississippi basin and upper Midwest (Small et al., 2006). From an ecosystems perspective, base flow is particularly important because it influences water temperatures in the summer and provides a minimum flow to sustain aquatic life. Climate model simulations indicate a shift toward higher winter flows and lower spring flows in New England (Campbell et al., 2011) and in the Great Lakes (Marshall and Randhir, 2008). In addition, short term soil moisture deficits, directly linked to the availability of water for agriculture and public water supplies, may also become more frequent (Hayhoe et al., 2007).

Several studies have identified the presence of changes in the mean and variance of observed streamflows in the region. McCabe and Wolock (2002) examine the maximum, mean, and minimum annual streamflows for the continental U.S. for the period of 1941–1999 and finds a step change in the mean and minimum values around 1970, suggesting that the climate system has shifted to a new regime with different statistical properties. Collins (2009) identifies a step change in the maximum annual observed flows around 1970 in 23 (out of 28) basins in New England (U.S.) and attributes those changes to the influence of the North Atlantic Oscillation's variability. The author also finds statistically significant upward trends in 40% of the basins. Conversely, changes in the mean and variance of flood peaks in 27% (40%) of the stations analyzed in the Eastern (Midwestern) U.S., have been attributed to changes in land use-land cover and might not be linked to climatic forcings (Villarini and Smith, 2010; Villarini et al., 2011).

Precipitation projections for the 21st century consistently indicate a wetter winter by the end of the century (Anderson et al., 2010; Hayhoe et al., 2007; Rawlins et al., 2012; Thibeault and Seth, 2014). For spring and fall, model projections agree on small positive changes in the Northeast U.S., which are significant over much of the region in spring and within the level of natural variability in the fall (Rawlins et al., 2012). In the Great Lakes region, winter and spring precipitation is projected to rise by as much as 20–30% before the end of the 21st century. Summer rainfall will experience no or little increase, which along with warmer temperatures, is likely to increase evapotranspiration and result in a net decrease of soil moisture storage in the region. Furthermore, declining snow pack can also reduce snowmelt recharge to groundwater reserves, which provides the water supply to sustain base flows during the summer (Hayhoe et al., 2008).

Although there have been several studies that evaluated temporal changes in streamflow properties for different sub-regions in the Northeast (NE) and Midwest (MW), to date no comprehensive region-wide analysis of the temporal trends in the future streamflow characteristics has been done. In this study, three streamflow characteristics are defined: 3-day peak flows, 7-day low flows, and mean base flows. The first two are particularly relevant to decision makers since peak flows impact the egg hatching of aquatic species while minimum flows propitiate healthy ecosystems and greatly impacts the municipal water supply during the warm summer months. The purpose of this paper is to investigate the magnitude, direction, and significance of temporal changes in streamflow characteristics in the NE–MW during the 20th and 21st centuries using climate-driven hydrologic simulations. Changes in the magnitude of the peaks and low flows will be evaluated for a 100-year return period. An additional goal is to identify the climate models that best represent the climatology of the region.

2. Data sources, models, and methods

2.1. Basin selection and observational data

The NE–MW region can be subdivided into four distinct climatic regions according to Fan et al. (2014): Region A (dry-cold), Region B (wet-cold), Region C (dry-warm), and Region D (wet-warm). Fig. 1a shows the spatial extent of each region.

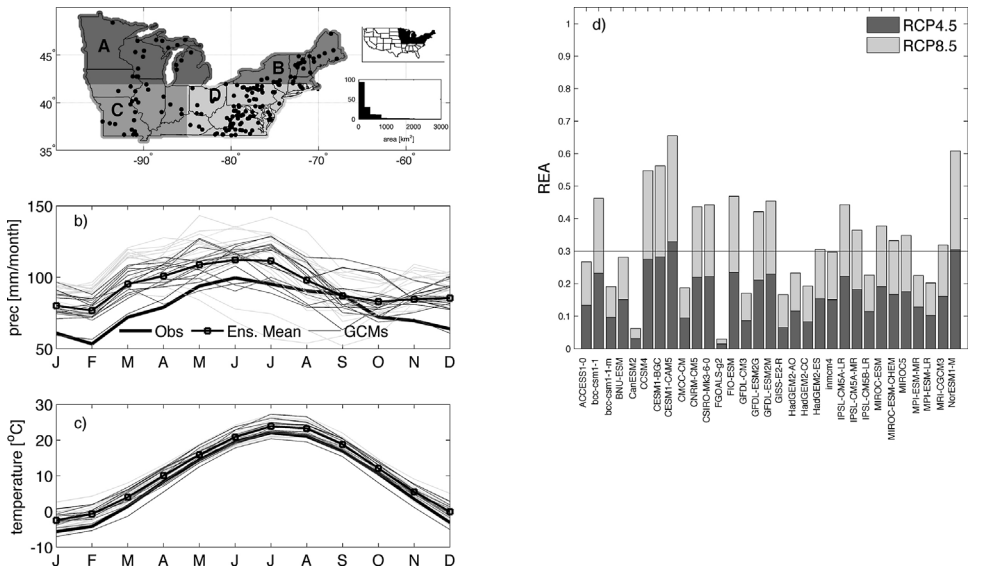

Fig. 1. (a) Geographical extend of the Northeast–Midwest (NE–MW) region and location of the basins selected for the study. Region A is dry-cold, Region B is wet-cold, Region C is dry-warm, and Region D is wet-warm. The insert shows the distribution of catchment's size. (b) Area averaged observed and GCM simulated precipitation climatology for the period 1901–2005, and (c) Area averaged observed and GCM simulated temperature. (d) Model reliability score (REA) for both precipitation and temperature averaged over the NE. Ranking based on closeness to historical observations (1901–2005) and to the ensemble average (2006–2099).

Basins with near-natural conditions, i.e., basins with no impoundments, flow diversions or other factors that could influence natural streamflows, were selected from the USGS Geospatial Attributes of Gages for Evaluating Streamflow (Gauges II) dataset (Falcone et al., 2010). For consistency, basins with 55 years of data during the period of 1950–2005 were selected. Additionally, basins were filtered to include only those that had at least 80% complete daily records. From the pool of available basins, 158 basins with drainage areas that range between 10 and 2500 km^2 (average 1000 km^2) met the two criteria (Fig. 1a).

Observed daily precipitation, maximum and minimum temperature at a 0.125° resolution for the conterminous U.S. were obtained from three datasets: (1) the North American Land Data Assimilation System version 2.0 (NLDAS-2, Xia et al., 2012) for the period of 1980–2008 was used by Princeton University to calibrate the VIC model, (2) the Maurer et al. (2002) dataset for the period of 1949–2005 was used to temporally disaggregate the climate simulations from monthly to daily values since its longer temporal record increases the number of observed events to be included in the analysis, and (3) monthly observed precipitation and temperature data from the Climate Research Unit (CRU) dataset for the period 1901–2005 (New et al., 2002) were selected to evaluate the skill of the climate models representing the historical climate of the region. Note that these three datasets are not independent since they share many of the rain gauges in the region and that the only reason behind their use was the different record lengths.

2.2. Streamflow simulations

The Variable Infiltration Capacity (VIC) model was used to simulate the streamflow of the 158 selected basins in the study area. The VIC model is a macro-scale hydrological model that represents surface and subsurface hydrologic processes in spatially distributed grids (Liang et al., 1994, 1996). VIC (version 4.0.6) was run in water balance mode at a daily time step, with a 3-h snow model, and a 0.125-degree spatial resolution. The VIC model calibrated parameters used in this study were obtained from Princeton University as described in Yuan et al. (2013). Briefly, VIC was calibrated using the method of Troy et al. (2008), which uses over 1700 USGS stream gauges and precipitation from the NLDAS-2 dataset, to create a monthly spatially-continued runoff field over the continental United States. The runoff field is then used to calibrate individual grid cells for the 1980–2004 period. The most common surface and subsurface VIC parameters: the infiltration parameter (b), the maximum baseflow generated in the deepest layer (D_m), the fraction of D_m where non-linear baseflow begins (D_s), the fraction of maximum soil moisture where non-linear baseflow is generated (W_s), and the thickness of soil layers 2 and 3 (D_2 and D_3, respectively) were calibrated for each 0.125-degree grid cell using the Shuffle Complex Evolution (SCE) algorithm (Duan et al., 1992). The objective function used for the optimization was the Kling–Gupta Efficiency (KGE, Gupta et al., 2009). All other soil, vegetation, and snow parameters were obtained from the LDAS dataset. In order to provide streamflow predictions at the 158 basins, the surface and subsurface generated runoff from VIC is routed using the channel routing scheme of Lohmann et al. (1998). The parameters for the routing model were calibrated independently from the VIC parameter calibration by using offline simulation of the calibrated VIC model forced by NLDAS-2. The wave velocity,

diffusivity, and the impulse response function were calibrated against the daily streamflow measurements from the USGS for each basin using the Shuffle Complex Evolution algorithm (Duan et al., 1992).

2.3. Future climate projections

In order to simulate the future streamflow characteristics in the basins using the VIC model, future climate projections from the Coupled Model Intercomparison Project Phase 5 archives (CMIP5, Taylor et al., 2012) were obtained at a 0.125° grid from the publicly available Bias Corrected and Statistically Downscaled WCRP CMIP5Climate Projections archive (Maurer et al., 2007) for two Representative Concentration Paths (RCPs): a mid-range concentration path (RCP 4.5) and a high concentration path (RCP 8.5). The dataset with climate projections can be accessed at http://gdo-dcp.ucllnl.org/downscaled_cmip_projections/dcpInterface.html. Several methods are available in the literature for removing biases in climate model simulations: Delta change, Quantile-Mapping, Analogue methods, Multiple linear regression (a more complete list of the methods can be found e.g., Themessl et al., 2011). We use a Quantile-Mapping approach (Panofsky and Brier, 1968) to bias-correct the monthly climate projections by matching their empirical probability distribution function to the observed. A spatial and a temporal disaggregation are performed to the bias-corrected fields. The spatial disaggregation consists of a linear interpolation that is applied to the anomalies of the monthly bias-corrected fields. The temporal disaggregation allows obtaining daily precipitation and temperature fields by randomly selecting observed daily time series from the historical climatology. For each month of the GCM (e.g., March, 2021) one month is randomly selected from the observations (e.g., February 1966) and used to disaggregate all the grid cells in the study area to be able to maintain the spatial structure of the storms. Each observed daily value is rescaled to match the climate simulated monthly total precipitation and average temperature using a multiplicative factor for precipitation and an additive factor for temperature. This method implicitly assumes that the day-to-day variability of future precipitation has been observed in the historical record; however the magnitude of the daily precipitation event is generated by the climate model and will change in time according to local and large-scale processes. This method has widely and successfully been used for hydrologic impacts studies (Brekke et al., 2004; Maurer et al., 2010b; Vano et al., 2014; Wood et al., 2004, 2002) and it has been shown to reproduce well extreme events and wet day frequencies at different spatial and temporal scales, however its skillfulness is limited to weather patterns observed during the historical period (Gutmann et al., 2014).

Additionally, raw, i.e., no spatial downscaling and bias correction, monthly precipitation and temperature fields were obtained from the CMIP5 archives (www.http://cmip-pcmdi.llnl.gov/). Since the main focus of this paper is on long-term trend analysis and the near future change, the analysis is performed in two 55-year periods: a historical period (1951–2005) and a future period centered around mid-century (2028–2082).

Multi-model ensembles have demonstrated increases in the skill and reliability of climate projections over a single-model projection (Tebaldi and Knutti, 2007), therefore the best performing General Circulation Models (GCMs) for the NE–MW were selected using a modified version of the Reliability Ensemble Average method (REA, Dominguez et al., 2010), which evaluates the GCM skills to simulate the present-day climate and the convergence of future climate to the ensemble average. The modified REA scores are computed as:

$$\mathrm{REA}_i = \mathrm{RP}_i \times \mathrm{RT}_i \tag{1}$$

where $\mathrm{RP}_i = \mathrm{R}_{H,i} \times \mathrm{R}_{F,i}$ and is a measure of reliability for precipitation and $\mathrm{RT}_i = \mathrm{R}_{H,i} \times \mathrm{R}_{F,i}$ is for mean temperature. In both cases, $\mathrm{R}_{H,i}$ measures model reliability in representing the historical climate (1901–2005) and $\mathrm{R}_{F,i}$ accounts for the convergence of each climate model to the REA average in the future (2006–2099). This does not imply that the REA represents the "true" future response for an emission scenario, but it represents the best estimated response (Giorgi and Mearns, 2002).

For each climate model, we computed the mean square error (MSE) between observed and simulated fields for the historical period, and between simulated fields and the REA-weighted average change for each month.

$$\mathrm{R}_{H,i} = \mathrm{MSE}(f, x) = \frac{1}{\mathrm{M}} \sum_{j}^{\mathrm{M}} \left(f_{j,i} - x_i\right)^2 \tag{2}$$

where $f_{j,i}$ represents the ith GCM for the month j. In the case of historical simulations x_j are regionally average observations. For the future period, $\mathrm{R}_{F,i}$ is computed with the same equation but in this case x_j is the REA-weighted average of the ensemble members for each month and it is computed as follows:

$$x_j = \frac{\sum_{1}^{\mathrm{N}} \mathrm{R}_i \times f_{i,j}}{\sum_{1}^{\mathrm{N}} \mathrm{R}_i} \tag{3}$$

To obtain a REA score where the largest values represent the best performing GCMs, $\mathrm{R}_{H,i}$ and $\mathrm{R}_{F,i}$ were normalized by the maximum value. For more details about the method the reader is referred to Dominguez et al. (2010).

2.4. Statistical methods

The use of moving averages in long-term trend analysis removes the effect of short-term oscillations or periodicities and minimizes the chance of selecting anomalously large or small values (Liuzzo and Freni, 2015). Three daily flow metrics were defined: the 3-day peak flow, the 7-day low flow, and the mean base flow (Das et al., 2011; Maurer et al., 2009; Risley et al., 2008). The 3-day flow peak is widely used for planning purposes, in particular in California and it has been widely in the literature for extreme analysis (Brekke et al., 2009; Das et al., 2011; Maurer et al., 2009, 2010a). The 7-day low flow is frequently used to characterize water quality and ecosystems impacts (Helsel and Hirsch, 2002; WMO, 2009), whereas the mean base flow characterizes the recession curve of the hydrograph and it is representative of groundwater contribution to stream runoff throughout the year (Sawaske and Freyberg, 2014).

To compute the first two metrics, first a 3-day and 7-day moving windows were applied to the data, and second the maximum and minimum values for each year were selected. Mean base flow was quantified through base flow separation using a low-pass filter parameter (Arnold and Allen, 1999; Carrillo et al., 2011), as follows:

$$Q_b(t) = \varepsilon Q_b(t-1) + \frac{1-\varepsilon}{2}[Q(t) - Q(t-1)] \tag{4}$$

where $Q(t)$ is the total streamflow at time t, Q_b is the computed base flow contribution to total flow, and ε is a low-pass filter parameter.

Since base flow can be highly correlated, hence masking the presence of a trend (Villarini and Smith, 2010), daily base flows were pre-whitened (i.e., remove unwanted correlations from the time series) with a process that removes a lag-one autoregressive (AR(1)) process from a time series (Douglas et al., 2000; Serinaldi and Kilsby, 2015), using the following formula:

$$Y(t) = Q_b(t) - r_1 Q_b(t-1) \tag{5}$$

where $Y(t)$ is the residual time series and r_1 is the lag one autocorrelation coefficient (Yue et al., 2002).

Statistically significant changes in the median of annual and seasonal precipitation, evapotranspiration, soil moisture, snow water equivalent (SWE), and streamflows were evaluated with the Wilcoxon (or Wilcoxon–Mann–Whitney) non-parametric test (Wilks, 2006). Changes (Δ) are estimated as:

$$\Delta = \left[\frac{(X_F - X_H)}{X_H}\right] \times 100 \tag{6}$$

where X represents the hydrological variable of interest for the future period of 2028–2082 (X_F), and for the historical period of 1951–2005 (X_H).

Step changes in the mean of streamflows were investigated with the Pettitt test (Pettitt, 1979) for each streamflow metric. The Pettitt test is a non-parametric test that does not make any assumptions about the functional form of the data distribution function. The magnitude of monotonic linear trends was evaluated with the Mann–Kendall (M–K) non-parametric test for each basin and for the GCM ensemble mean. The magnitude of the trends was estimated with the Sen's method (Kendall, 1975; Mann, 1945; Sen, 1968). The statistical significance of the results was evaluated at a 0.05 significance level. No hinge trend analysis was carried out (Livezey et al., 2007), hence only basins without detected changes in the mean were included in the trend analysis.

Changes in the frequency (events per year) of daily flows above/below the baseline 90th/10th percentile were evaluated for each basin (Hayhoe et al., 2007). Changes in the length of the low flow (summer) season in the future were analyzed by selecting the number of days below the 10th percentile for each basin.

To evaluate if the magnitude of flow peak is likely to increase in the 21st century as a result of the projected climate change, a Generalized Extreme Value (GEV) distribution function (Das et al., 2011; Hurkmans et al., 2010; Maurer et al., 2009) was fitted to the ensemble mean annual 3-day peak flows and the model parameters were estimated with the maximum likelihood method (Coles, 2001).

$$G(z) = \exp\left\{-\left[1 + \xi\left(\frac{z-\mu}{\sigma}\right)\right]^{\frac{-1}{\xi}}\right\} \tag{7}$$

where μ is the location parameter, σ is the scale parameter and ξ is the shape parameter.

Similarly, a Weibull theoretical distribution was fitted to the annual 7-day low flows ensemble mean (Maurer et al., 2009; Vicente-Serrano et al., 2012). The Weibull distribution is a special case of Eq. (7) when the shape parameter (ξ) is <0.

3. Climate and hydrological models validation

3.1. GCM performance for the study area

The skill of GCMs representing the climatology of the NE–MW was evaluated by comparing the raw GCMs (before bias correction) to the observed fields from the CRU dataset during the period of 1901–2005, and the individual GCM convergence to the REA average in the future climate simulations. GCM and CRU monthly precipitation and temperature were averaged

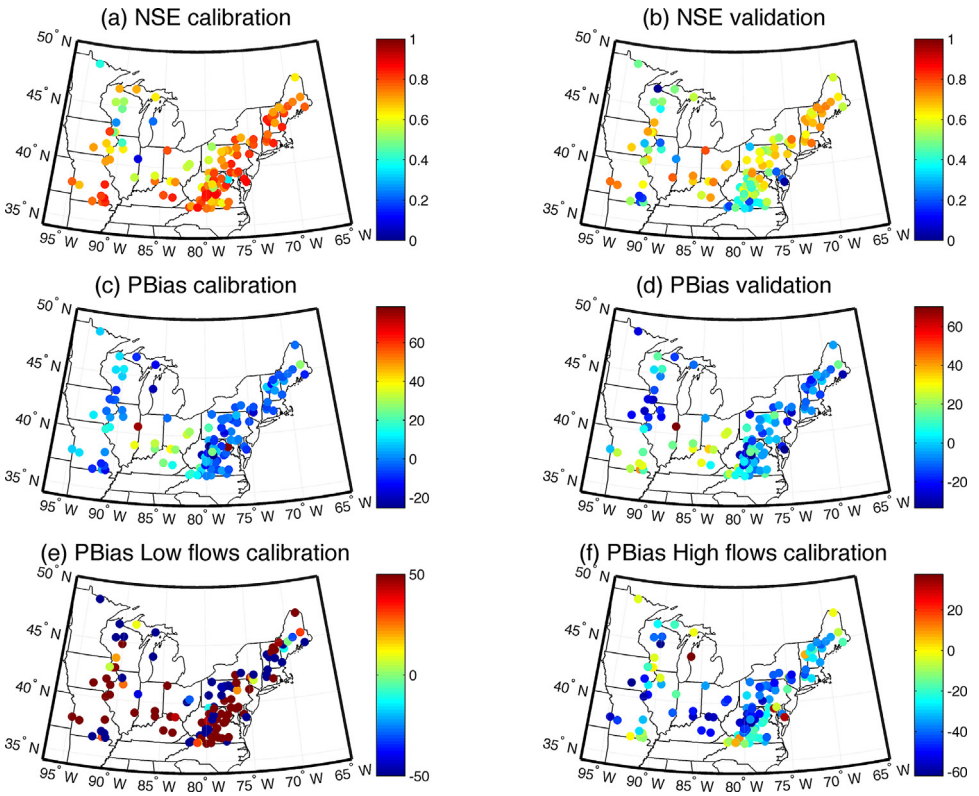

Fig. 2. Monthly VIC model performance for the calibration period (1980–2004) and validation period (2005–2010) for the 124 basins included in the study. Nash–Sutcliffe Efficiency (a) and (b) and Percent bias (Pbias) in% (c) and (d). Panels show the Pbias (e) for daily flows above the 98th percentile and (f) daily flows above the 70th percentile.

for the study region. It is worth noting that higher spatial resolution precipitation and temperature products are available for the conterminous U.S., however the CRU dataset has shown comparable results to PRISM (Daly et al., 1994) for the region (Fan et al., 2014; Fan and van den Dool, 2008; Nag et al., 2014).

Fig. 1b and c shows that the observed precipitation is overestimated by the climate model ensemble-mean, whereas ensemble mean temperature is closer to the observations. The sixteen best performing models, selected with a combined (RCP 4.5 + RCP 8.5) REA score of 0.3 average for the region, are shown in Fig. 1d: bcc-csm1-1, CCSM4, CESM1-BGC, CESM1-CAM5, CNRM-CM5, CSIRO-Mk3-6-0, FIO-ESM, GFDL-ESM2G, GFDL-ESM2M, IPSL-CM5A-LR, IPSL-CM5A-MR, MIROC-ESM, MIROC-ESM-CHEM, MIROC5, MPI-ESM-LR, and NorESM1-M.

3.2. VIC validation

The VIC model was forced with daily observed precipitation, maximum and minimum temperature from the NLDAS-2 dataset from 1980 to 2010 (the reader is referred to Yuan et al., 2013 for details). Calibration (1980–2004) and validation (2005–2010) statistics at the monthly and daily levels are shown in Fig. 2. From the originally selected 158 basins, 34 reported negative Nash–Sutcliffe Efficiency values (NSE) and were excluded from the analysis to ensure a reasonable representation of the climate-streamflow characteristics of the basins. Fig. 2 shows NSE and the relative bias (Pbias) of the monthly streamflows during the calibration and validation periods. During the calibration period the average NSE for the 124 basins was 0.70($\pm$0.14) and the Pbias was 2.50($\pm$16.6)% which meet the criteria for "satisfactory" calibration by Moriasi et al. (2007). For the validation period, the NSE and Pbias deteriorate to 0.61($\pm$0.25) and $-1.97(\pm17.9)$%, respectively. Since the study focuses on extremes, Fig. 2e and f shows the Pbias for daily flows exceeded 2% of the time and 70% of the time in any given year following recommendation by Yilmaz et al. (2008). VIC simulated low flows overestimated observations in most of the region whereas peak flows were systematically underestimated. This is not surprising since VIC was calibrated to match monthly values and it is quite likely that the low performance is due to a differences in the timing of the peaks. Similar limitations using VIC for basins in New England have been reported by Hayhoe et al. (2007). The Proportions test (King and Mody, 2010) was used to evaluate if the proportion of daily observed and simulated streamflows below/over the 70th/98th percentile was equal in both samples. The null hypothesis H_0 states that both population proportions are equal to p. The proportion (p), average for the 124 basins, of daily streamflows below the 70th threshold was found to be 0.613($\pm$0.29) and 0.612($\pm$0.29) for observations and simulations during the calibration period, respectively. The Z-test was used to measure

Table 1
Model names and hosting institutions used in this study. Only best performing models are included.

	Model	Modeling center
1	bcc-csm1-1	Beijing Climate Center, China Meteorological Administration
2	CCSM4	National Center of Atmospheric Research, USA
3	CESM1-BGC	Community Earth System Model Contributors
4	CESM1-CAM5	Community Earth System Model Contributors
5	CNRM-CM5	National Centre of Meteorological Research, France
6	CSIRO-mk3-6-0	Commonwealth Scientific and Industrial Research Organization/Queensland Climate Change Centre of Excellence, Australia
7	FIO-ESM	The First Institute of Oceanography, SOA, China
8	GFDL-ESM2G	NOAA Geophysical Fluid Dynamics Laboratory, USA
9	GFDL-ESM2M	NOAA Geophysical Fluid Dynamics Laboratory, USA
10	IPSL-cm5a-lr	Institut Pierre Simon Laplace, France
11	IPSL-cm5a-mr	Institut Pierre Simon Laplace, France
12	MIROC-esm	Japan Agency for Marine-Earth Science and Technology, Atmosphere and Ocean Research Institute (The University of Tokyo), and National Institute for Environmental Studies
13	MIROC-esm-chem	Same as MICOC-esm
14	MIROC5	Same as MIROC4h
15	MPI-ESM-LR	Max Planck Institute for Meteorology, Germany
16	NORESM1-m	Norwegian Climate Center, Norway

the statistical significance of the differences at a 5% level. The associated Z value was 0.169($\pm$0.28) which is within the $<\pm 1.96$ limits of a $N(0,1)$ distribution. For peak flows, the proportion was 0.0164($\pm$0.0078) for both samples with an average Z value equal to 0.0356($\pm$0.0594), respectively. For low and peak flows, the hypothesis of difference in the proportion of daily events below/above the threshold cannot be rejected at the significance level indicating that the VIC model can realistically capture the occurrence of extreme flows in the basins.

4. Results and discussion

In this section, we will evaluate the future projected changes in hydrological variables, and whether the magnitude of peak and low flows is likely to increase during the 21st Century. First, daily streamflows are simulated in the 124 basins using daily precipitation and temperature for each of the sixteen GCMs. Second, for each basin the GCM ensemble-mean is computed; and third to make the magnitude of the trends comparable between basins, specific discharges are computed by dividing 3-day, 7-day, and mean base flows by the respective basin areas (Table 1).

4.1. Changes in annual and seasonal hydrologic states and fluxes

We begin our evaluation by comparing the future changes in ensemble-mean seasonal fluxes (i.e., evapotranspiration, slow response flow, fast response flow) and states (i.e., soil moisture and snow water equivalent (SWE)) for each sub-region (Table 2) between the future and historical periods. The seasons are defined as: Winter (December–January–February), Spring (March–April–May), Summer (June–July–August), and Fall (September–October–November). For each basin, first precipitation and evapotranspiration are summed over the analysis period whereas temperature, soil moisture, SWE, slow response flow, and fast response flow are averaged. Second, each hydrologic variable is averaged for the basins located in each region: Region A contains 15 basins; Region B, 22 basins; Region C, 21 basins; and Region D, 68 basins. The statistical significance of the changes was tested with the Wilcoxon test. Regions A, B, and D will experience the largest increases in precipitation in Winter and Spring ranging from 9.8% to 13.6%; while in Region C the increases will range from 8.3% to 10.8%. In average for the four regions, Summer precipitation is expected to increase by mid-century, by 7.9/7.2% in the RCP 4.5/RCP 8.5 scenarios, respectively. During the Fall, the eastern basins will receive slightly more precipitation than the western basins. Changes in temperatures will be evenly distributed in all four regions with changes ranging from 2.3 °C to 2.9 °C in the mid-range emission scenario and between 2.9 °C and 4.0 °C in the high emission scenario.

Evapotranspiration will likely increase throughout the year in all four regions with the exception of the Winter season in the northern basins (Region A and B), perhaps due to less sublimation from reduced snow packs. Coincidently, SWE shows the largest negative changes during the cold season in the two regions from -15.7 to -31.8 mm day^{-1}/seas for RCP 4.5 and from -19.9 to -41.8 mm day^{-1}/seas for RCP 8.5. Larger evaporation rates during the warm months (Summer and Fall) are likely to reduce soil moisture storage and minimize slow response runoff generation in order satisfy the atmospheric water deficit. Finally, fast response runoff (fast model response to precipitation when the upper soil layer saturates) is projected to increase in the Winter months as a response to more rainfall.

Table 2
Changes in future (2028–2082) seasonal fluxes and states for the 4 climatic regions in the NE–MW: Region A (dry-cold), Region B (wet-cold), Region C (dry-warm) and Region D (wet-warm). Hydrologic components are averaged only for the basins included in each climatic region. Numbers in parentheses indicate not statistically significant changes (α 0.05).

	Region	A	B	C	D	A	B	C	D
	Units	RCP 4.5				RCP 8.5			
Precipitation	%								
DJF (winter)		11.6	10.4	8.3	12.5	13.6	12.6	9.2	11.3
MAM (spring)		9.8	7.1	10.1	9.1	13.1	12.7	10.8	12.0
JJA (summer)		6.4	7.3	8.9	9.0	5.1	8.5	7.6	7.6
SON (fall)		6.6	8.8	6.9	8.6	5.0	6.5	8.1	7.1
Temperature	°C								
DJF (winter)		2.7	2.9	2.3	2.7	3.8	4.0	3.1	3.6
MAM (spring)		2.6	2.6	2.3	2.6	3.2	3.3	2.9	3.2
JJA (summer)		2.5	2.5	2.5	2.5	3.4	3.4	3.3	3.3
SON (fall)		2.6	2.5	2.6	2.6	3.3	3.3	3.3	3.3
Evapotranspiration	mm day^{-1}/seas								
DJF (winter)		−0.7	(−0.2)	4.9	1.8	−1.0	−0.6	6.8	2.3
MAM (spring)		11.9	11.7	14.5	14.0	16.0	15.3	20.6	18.1
JJA (summer)		17.8	19.2	19.5	18.7	21.4	25.2	20.9	22.0
SON (fall)		11.0	12.3	13.1	13.6	13.2	15.3	14.9	14.5
Soil moisture	mm day^{-1}/seas								
DJF (winter)		2.2	4.3	1.2	2.4	2.2	5.3	0.4	2.3
MAM (spring)		(0.1)	(−0.2)	(0.2)	(0.2)	(0.2)	(−0.1)	(0.1)	(0.0)
JJA (summer)		(−0.5)	−1.1	(−0.3)	(−0.2)	−1.4	−1.8	−1.6	−1.4
SON (fall)		(−0.5)	(−0.6)	(−0.2)	(0.0)	−1.8	−2.3	−1.6	−1.2
SWE	mm day^{-1}/seas								
DJF (winter)		−15.7	−31.8	−5.8	−17.0	−19.9	−41.8	−7.3	−21.4
MAM (spring)		−5.9	−33.7	−1.8	−13.4	−6.9	−40.6	−2.1	−15.9
JJA (summer)		0.0	−0.1	0.0	0.0	0.0	−0.1	0.0	0.0
SON (fall)		−0.2	−0.5	−0.1	−0.2	−0.2	−0.6	−0.1	−0.3
Slow response flow	mm day^{-1}/seas								
DJF (winter)		0.4	0.6	0.2	0.3	0.4	0.8	0.1	0.4
MAM (spring)		(0.0)	−0.2	(0.0)	0.0	(0.0)	−0.2	(0.1)	−0.1
JJA (summer)		(0.0)	(0.0)	(0.0)	(0.0)	(0.0)	(0.0)	0.0)	(0.0)
SON (fall)		(0.0)	(0.1)	(0.0)	0.1	−0.1	(0.0)	(0.0)	(0.0)
Fast response flow	mm day^{-1}/seas								
DJF (winter)		0.3	0.3	0.1	0.2	0.4	0.4	0.1	0.2
MAM (spring)		(0.0)	−0.1	0.1	(0.0)	(0.0)	−0.1	(0.0)	(0.0)
JJA (summer)		0.0	0.0	0.1	0.0	(0.0)	(0.0)	(0.0)	(0.0)
SON (fall)		0.1	0.1	0.1	0.0	(0.0)	(0.0)	0.1	(0.0)

4.2. Trends in precipitation and streamflows

Given the high dependence on the frequency, intensity, and timing of extreme precipitation and streamflows for water resources sustainability, a primary need is to estimate the potential changes in the temporal and spatial variability of extreme events due to a changing climate. The frequency of very heavy precipitation (101.6 mm or 4 in.) has increased in the region during the last century (Changnon and Westcott, 2002; Douglas and Fairbank, 2011; Groisman et al., 2001; Mishra and Lettenmaier, 2011), perhaps as a result of warmer atmospheric temperatures which increased the atmospheric water vapor holding capacity (Trenberth et al., 2003). Since antecedent precipitation in a catchment is more likely to be related to large peaks than a single isolated precipitation event, first we computed the maximum 5-day cumulative precipitation following the U.S. Natural Resources Conservation Service (NRCS, 2004) recommendations for rainfall-runoff estimations for each GCM and each basin. Second, the maximum 5-day value was selected for each year in the 1951–2099 period; and third, the presence of linear trends in the GCM ensemble-mean was assessed with the Mann–Kendall test with a 0.05 significance level.

Fig. 3 shows trends in the annual maximum cumulative 5-day precipitation for the GCM ensemble-mean during the historical period (left panel), and for the future period (center and right panels). Upward/downward pointing triangles indicate positive/negative trends, with colored markers showing statistically significant trends. The percentage of cases with statistically significant positive and negative trends in the 55-year period is noted between brackets. Mostly, positive changes result from the simulated GCM 5-day maximum precipitation with statistically significant trends restricted to the western part of the domain. By mid-century, GCM ensemble-mean precipitation is projected to be more intense in the eastern part of the U.S. (Regions B and D) under both concentration paths with 22% of the basins showing statistically significant upward trends.

Change point analysis of the observed 3-day peak flows using the Pettitt test shows changes in the mean in 14% of the basins at a 5% confidence level (Fig. 4a). Most of the basins are located in the western part of the domain and a few basins in the southeastern corner. The median value of the change date is 1978 with a standard deviation of ±8 years. The number of basins with identified changes in the mean increases to 31% for the ensemble mean of GCM-driven maximum flows (Fig. 4d) with most of the basins located in the eastern region. For 7-day low flows, observations show that 32% of the basins have a change in mean around the year 1974 (±13 years), whereas for GCM-driven simulations only 14% of the basins experience statistically significant changes (Fig. 4e). Mean observed base flows report changes in the mean in 19% of the basins occurring around the year 1979(±11 years). Basins with detected changes tend to be concentrated in the western part of the domain. Conversely, GCM-driven VIC simulations show 73% of the basins having changes in the mean in the year 1983(±10 years). In all cases, the observed year of the detected changes in mean is, in average, slightly later in the 20th Century than the dates reported in previous studies (Villarini and Smith, 2010). Perhaps the differences arise from the length of the flow records used in this study, which spans 55 years, whereas the aforementioned study used longer records. These differences could be due to deficiencies in the climate model simulating the inter-annual variability of precipitation in the region (the 1960's drought significantly impacted these values (Hayhoe et al., 2007; Namias, 1966)). During this intense drought, changes in moisture fluxes and in the position of the storm tracks in the northeast U.S. were the result of a negative North Atlantic Oscillation (NAO) pattern, la Niña conditions, and a negative Pacific–North American (PNA) pattern (Ning and Bradley, 2014), and might have influence the trend of hydrological variables (Hayhoe et al., 2007).

The presence of linear trends in ensemble-mean 3-day peak flows, 7-day low flows, and mean base flows was evaluated for each basin with the Mann–Kendall test. Fig. 5 shows the direction of the trend GCM-driven streamflow characteristics during the historical (1951–2005) and the future (2028–2082) periods in those basins where no point changes in the mean were found with the Pettitt test (Fig. 4). During the historical period, the ensemble mean GCM-driven 3-day peak flows show widespread positive trends throughout the region, however only 6% basins exhibit statistically significant trends (Fig. 5a). Climate projections for the period of 2028–2082 for both concentration paths show positive trends in the eastern half of the study area (Fig. 5b) and negative trends in the western side of the domain (Regions A and D) for the mid-range mitigation scenario. Under the high emission scenario, more intense precipitation (Fig. 3) might be linked to significant changes toward larger peak flows in the eastern half with the exception of the far northeastern U.S. (Maine) where peak flows show a downward trend. These pattern involving decreasing peak flows despite a projected intensification in precipitation could be linked to: (1) projected decreases in snow cover during the winter–spring season which will impact the magnitude of peak flows. During the historical period, peak flows occur, in average for the ensemble mean, during the spring season (Julian

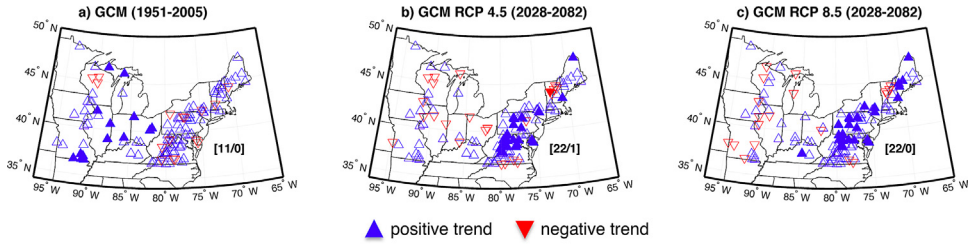

Fig. 3. Linear trends in annual maximum cumulative 5-day precipitation for the GMC ensemble-mean: (a) historical period (1951–2005), (b) RCP 4.5 future period (2028–2082), and c) RCP 8.5 future period (2028–2082). Statistically significant trends are shown with filled triangles (α 0.05). Upward pointing triangles indicated positive trends and downward pointing ones denote negative trends.

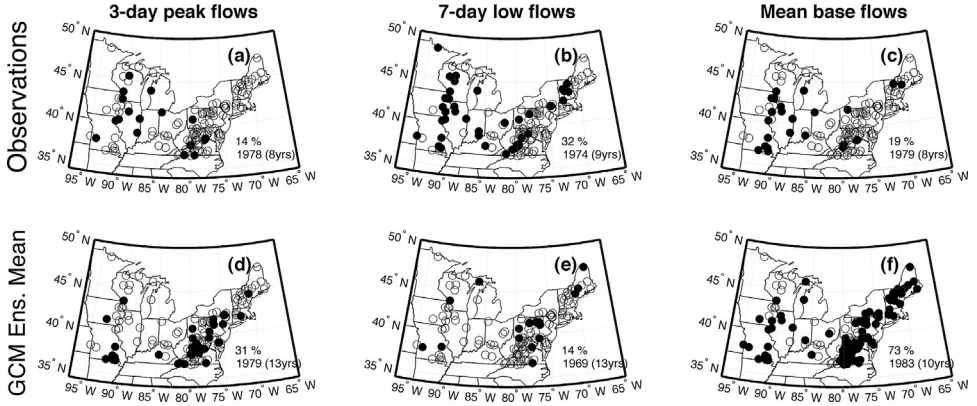

Fig. 4. Spatial distribution of basins with changes in the mean (Pettitt test) in observations (top row) and ensemble mean of GCM-driven simulations (bottom row): 3-day peak flows, 7-day low flows, and mean base flows. The numbers in the lower right corner indicate the percentage of basins with statistically significant changes at the 5% confidence level, and the median and standard deviation of the year when the change was detected.

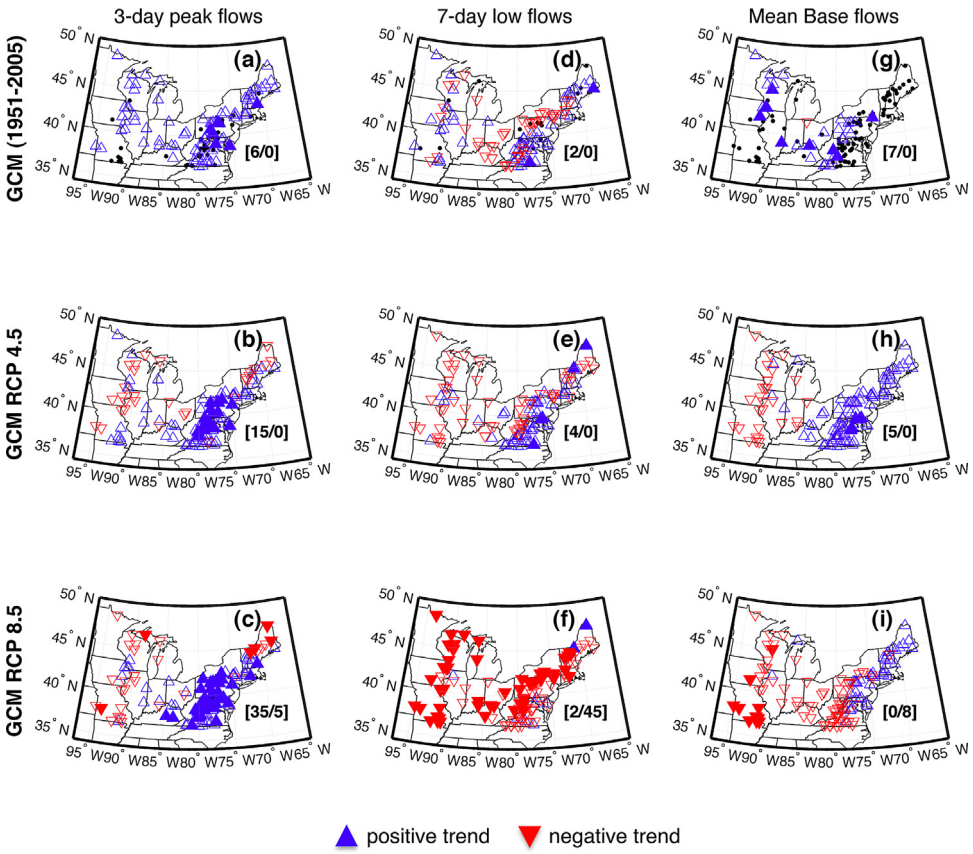

Fig. 5. Trends in GCM-driven simulations of 3-day peak flows (left column), 7-day low flows (middle column), and annual pre-whitened mean base flows (right column), during the historical (1951–2005) and future (2028–2082) periods. The black dot indicates the location of basins with statistically significant (α 0.05) point changes in the mean using the Pettitt test in Fig. 4. The numbers in the lower right corner indicate the percentage of basins with statistically significant trends.

day 120 ± 70 days). Climate projections for the 21st century show a negative trend in the date of the 3-day peak flows of 0.055 days/year for the RCP 4.5 path, which suggests changes in snow melting as atmospheric temperatures increase; and (2) the seasonality of the extremes since climate model simulations indicate that maximum precipitation intensities occur in late summer (Julian day 220 ± 80 days) therefore the increases in storm intensity shown in Fig. 3 might not be related to increases in channel runoff. A follow up study will evaluate changes in precipitation and streamflow characteristics at the seasonal level. Overall, 35/5% basins will experience positive/negative trends by mid-century.

Annual 7-day low flows show a mix of positive and negative trends across the domain with most of them being not statistically significant (Fig. 5d). Increasing trends in 4% of the basins are projected for the GCM-ensemble for 7-day low flows by mid-century with most of the basins located in the eastern half of the domain (Fig. 5e). Under the high emission scenarios, climate model simulations yield widespread negative trends in the region with only 2 basins having statistically robust positive trends (Fig. 5f). Changes in the magnitude and duration of future summer–fall low flows in the Northeast US has been documented by Hayhoe et al. (2007), suggesting that even with the projected increase in precipitation during the winter months and small changes during the warm months, we are likely to experience more dramatic low flow conditions.

Annual mean base flows show not statistically robust positive trends in the eastern half of the domain (Regions B and D) and negative trends in Regions A and C under the RCP 4.5 concentration path (Fig. 5h). This positive trends can be linked to increasing summer precipitation or to increased aquifer recharge due to earlier snow melting or to more rain falling as liquid in the cold months. By mid-century, negative trends are likely to be found in most of the domain under the RCP 8.5 concentration path with 8% of the basins showing statistically significant trends in Regions A and C (Fig. 5i).

For each 55-year period, a GEV distribution function was fitted to the time series of 3-day peak flows and the inverse of the probability was computed for the 100-year return period. It is worth noticing that stationarity in the GEV parameters was assumed. Percentage changes between future and historical projections are mostly positive throughout the region with changes reaching up to 40% under the RCP 8.5 concentration path (Fig. 6a and b). Interestingly, negative changes are projected for part of Region B (northeastern U.S.), which is in agreement with the trend analysis shown in Fig. 5. Similarly, for 7-day low flows a Weibull distribution was fitted to the data. Fig. 6c and d show a projected decrease in the magnitude of low flows by mid-century of up to 90% under the RCP 8.5 concentration path.

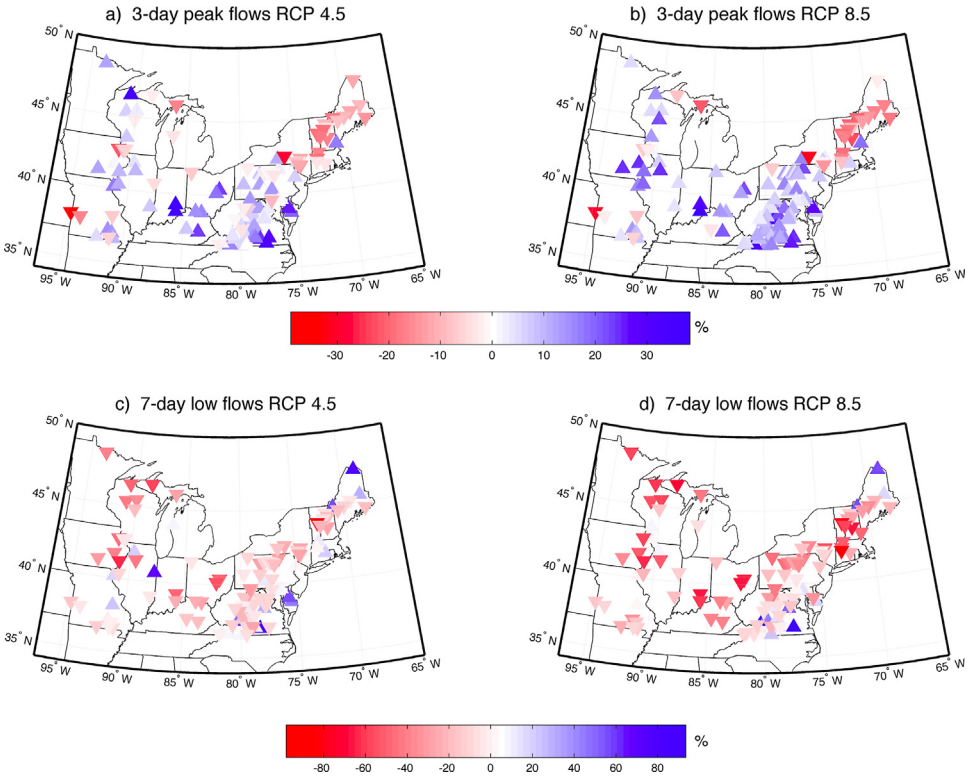

Fig. 6. Percentage changes in the magnitude of the 100-year return period 3-day peak flow (top panels) and 7-day low flows (bottom panels). Changes are expressed as percentage changes from the historical period (1951–2005).

Table 3
Ensemble mean frequency (events/year) of daily flows above/below the 90th/10th baseline percentile. Frequencies are average for all the basins in each climatic Region. Streamflow simulations, forced with the mid-range (RCP 4.5) and high (RCP 8.5) concentration path, are compared to the historical period. The number between parentheses represents the percent change from the historical period.

	1951–2005	2028–2082	
(a) Peak Flows	Historical	RCP 4.5	RCP 8.5
Region A (dry-cold)	39.9	48.1(+20.7)	49.2(+23.5)
Region B (wet-cold)	41.2	46.1(+11.7)	48.9(+18.7)
Region C (dry-warm)	42.3	50.3(+18.9)	49.8(+17.7)
Region D (wet-warm)	40.8	48.4(+18.5)	48.7(+19.1)
(b) Low Flows			
Region A (dry-cold)	16.4	19.2(+17.6)	20.9(+27.8)
Region B (wet-cold)	22.6	21.9(−3.2)	20.7(−8.4)
Region C (dry-warm)	23.5	24.9(+5.9)	22.5(−4.3)
Region D (wet-warm)	20.2	20.4(+0.8)	23.0(+13.6)

4.3. Extreme flow events at mid-century: will they become more frequent?

To further evaluate how high and low flow events will be impacted by anthropogenic-induced changes in climate an over-the-threshold analysis is conducted on daily streamflows for each of the selected GCMs. In contrast to the annual extreme analysis used in the previous sections, this method includes all the streamflow values that are above or below a set threshold allowing a larger sample size. To select the streamflows, first we determine the 10th and 90th percentiles from the observation-driven VIC simulations. Second, we compute the frequency (events per year) of daily flows above/below the 90th/10th percentile for each basin and each GCM during the historical and the future periods. Third, we obtain the frequencies (events per year) mean and standard deviation for each climatic region and we average them for all the climate models. Table 3a shows that the ensemble mean GCM simulations under the RCP 4.5 scenario yield increases in daily peak flows in all regions by mid-century ranging from 11% to 20% (percentages are expressed with respect to the historical period). Under the RCP 8.5 scenario, increases range from 17% to 23% indicating that despite the negative trends in annual maximum flows found for the western region (Fig. 6a and b), flooding events of a moderate magnitude will be more frequent in the future. Similarly, daily flows below the 10th percentile, i.e., low flow conditions, will become more frequent in Regions A, B, and D under the RCP 4.5 scenario with the largest changes expected to occur in the wetter basins. The number of days with

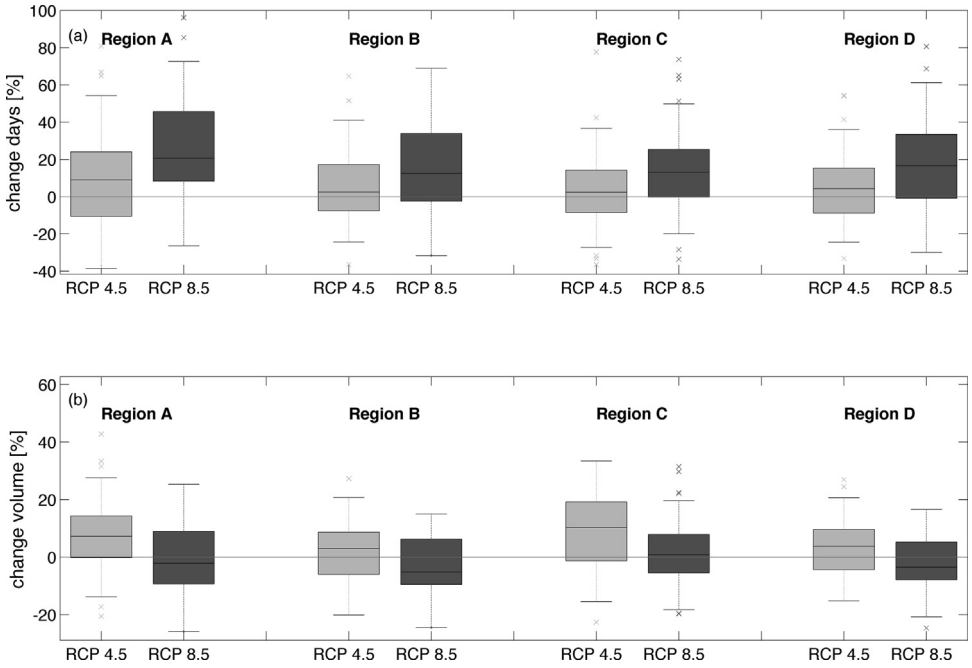

Fig. 7. (a) Change in the number of days with flows below the observed 10th percentile and (b) Changes in flow volumes. Results are valid for the low flow season defined as May 1st and October 31st. Changes are computed between the future (2028–2082) period and the historical period.

low flow conditions will increase between 0.8 and 17.6%. Under the RCP 8.5 scenario, negative changes in Regions B and C suggests that after evapotranspiration demand is met, excess precipitation contributes to flow generation or soil moisture content in the basins.

Since summer and fall flows are vital for ecosystem functioning, water supply and hydroelectric purposes, we assess whether the length of low flow condition will extend in the future. For each basin, the number of daily flows below the 10th percentile during the low flow season (May 1st to October 31st) are computed and subsequently averaged for each region. Under the RCP 4.5 pathway the length of the low flows season will increase, in average, by 6% for the four climatic regions with respect to the historical period (Fig. 7a). Changes under RCP 8.5 are larger, 18% on average, for all basins indicating that despite the projected increased in precipitation low flow conditions will still prevail in the basins as water demand increases during the warm months. The length of the low flow season will extend, in average, by 5 ± 3 days under warmer climate conditions by mid-century (statistically significant at the 95% significance level).

Additionally, we compute the yearly total flow volume for the 184 days between May and October for each basin and each climate model to evaluate if, despite the increase in the number of low flow conditions, the volume of water in the channel will be affected. Results indicate a slight increase of flow volumes in the future under the RCP 4.5 scenario perhaps as a result of intense precipitation events which will bring more frequent high flow conditions (Fig. 7b). Conversely, volumes will slightly decrease for RCP 8.5 (changes not statistically significant) despite projected precipitation increases during spring, summer, and fall (Table 2). During the warm period, larger evapotranspiration rates associated to warmer temperatures will likely contribute to lower water levels in the channels which will potentially affect aquatic and human ecosystems.

5. Conclusions

Our work investigates the projected trends and changes on streamflow characteristic in the Northeast–Midwest U.S. during the 20th and 21st centuries. We selected 124 basins throughout the region to assess trends in 3-day peak flows, 7-day low flows, and mean base flows by mid-century. Spatially disaggregated and bias-corrected precipitation and temperature fields for sixteen well performing climate models from the CMIP5 Project and for two future concentration paths were used as an input to the VIC hydrological model. Simulations were compared between two 55-year periods: the historical (1951–2005) and a future centered at mid-century (2028–2082).

Changes in the annual cycle of precipitation are projected to occur during the 21st century with increases in winter precipitation and small positive changes in summer precipitation. The northern basins will experience larger increases of precipitation, whereas temperature increases will be spatially distributed across the region. Declining snow packages, despite increased winter and fall precipitation, is likely to occur across the entire domain due to higher snow-melting and sublimation rates or perhaps due to changes in rainfall phase as documented in the Western U.S. (Barnett et al., 2005).

Spatial analysis indicates that annual maximum 5-day precipitation is projected to have robust positive trends in the eastern half of the region by mid-century. Similarly, simulations show that the magnitude of 3-day peak flows is likely to increase across the eastern side of the region as a result of more intense precipitation events whereas the western region is likely to experience decreases. Positive future changes in the 100-year 3-day flows are likely to dominate the NE–MW region by mid-century.

Regional declining trends in 7-day low flows under the RCP8.5 concentration path are projected for the GCM ensemble-mean, whereas negative trends in mean base flows will likely be frequent in the west. Negative changes in the magnitude of the 7-day low flows with a 100-year return period will be widespread throughout the region.

The frequency (events per year) of daily low flows (below the observed 10th percentile) and peak flows (above the observed 90th percentile) is likely to increase across the region, and the length of the low flow season is likely to extend under the RCP 8.5 concentration path as water demands increase. By mid-century, projected streamflow simulations using 16 climate models show a decrease in river channel volumes during the warm months.

Selection of climate models for the region, based on how well they reproduce observations and how close future simulations are to the ensemble-mean, can reduce simulation uncertainty. However, the uncertainty in GCM projections due to their coarse spatial resolution is not reduced with statistical downscaling making the use of Regional Climate Models an attractive alternative for future studies as they become more widely available (Liang et al., 2012). Furthermore, structural biases in the hydrological models and uncertainty in the bias correction–temporal disaggregation process can contribute to underestimation of streamflow extremes, which implies that mid-century projected positive trends can be a conservative estimate of their magnitude. Low flows conditions on the other hand will likely be less pronounced. However, there are two caveats. First, VIC simulations assume that the vegetation cover is static in time, therefore the interaction between snow and vegetation might not be realistically represented in the future. Second, VIC model structure assumes model transportability in time hence the parameter calibration will be valid under different climatic conditions.

Based on our results, it is evident that under the current warming trend, different natural and social economic factors will be affected by extreme streamflow events, and by low flow conditions during the crucial warm season. Thus, wildlife managers, water managers, and decision makers in the region may need to adapt to less water availability during the warmer months; and as peak flows become more extreme, efforts should be directed at quantifying their impact on existent infrastructure and on riverside human settlements due to erosion processes and flooding.

Acknowledgments

This study was funded by USGS-DOI Grant #111-1485 to the Northeast Climate Science Center at the University of Massachusetts, Amherst. The authors are grateful to WCRP for its role in making available the CMIP5 dataset, to Dr. Daniel A. Rodriguez at CPTEC for his advice with the statistical methods, and to Dr. Austin Polebitski and Dr. Scott Steinschneider for their help with the Gauges II database. We would like to thank the editor and two anonymous reviewers whose comments substantially improved the quality of the paper.

Appendix A. Supplementary data

Supplementary data associated with this article can be found, in the online version, at http://dx.doi.org/10.1016/j.ejrh.2015.11.007.

References

Anderson, B.T., Hayhoe, K., Liang, X.Z., 2010. Anthropogenic-induced changes in twenty-first century summertime hydroclimatology of the Northeastern US. Clim. Change 99 (3–4), 403–423.
Armstrong, W.H., Collins, M.J., Snyder, N.P., 2012. Increased frequency of low-magnitude floods in New England. J. Am. Water Resour. Assoc. 48 (2), 306–320.
Arnold, J.G., Allen, P.M., 1999. Automated methods for estimating baseflow and ground water recharge from streamflow records. J. Am. Water Resour. Assoc. 35 (2), 411–424.
Barnett, T.P., Adam, J.C., Lettenmaier, D.P., 2005. Potential impacts of a warming climate on water availability in snow-dominated regions. Nature 438 (7066), 303–309.
Brekke, L.D., Miller, N.L., Bashford, K.E., Quinn, N.W.T., Dracup, J.A., 2004. Climate change impacts uncertainty for water resources in the San Joaquin River Basin, California. J. Am. Water Resour. Assoc. 40 (1), 149–164.
Brekke, L.D., et al., 2009. Assessing reservoir operations risk under climate change. Water Resour. Res. 45, W04411.
Brown, P.J., Bradley, R.S., Keimig, F.T., 2010. Changes in extreme climate indices for the Northeastern United States, 1870–2005. J. Climate 23 (24), 6555–6572.
Campbell, J.L., Driscoll, C.T., Pourmokhtarian, A., Hayhoe, K., 2011. Streamflow responses to past and projected future changes in climate at the Hubbard Brook Experimental Forest, New Hampshire, United States. Water Resour. Res. 47, W02514.
Carrillo, G., et al., 2011. Catchment classification: hydrological analysis of catchment behavior through process-based modeling along a climate gradient. Hydrol. Earth Syst. Sci. 15 (11), 3411–3430.
Changnon, S.A., Westcott, N.E., 2002. Heavy rainstorms in Chicago: increasing frequency, altered impacts, and future implications. J. Am. Water Resour. Assoc. 38 (5), 1467–1475.
Changnon, S.A., 2002. Frequency of heavy rainstorms on areas from 10 to 10,000km(2), defined using dense rain gauge networks. J. Hydrometeorol. 3 (2), 220–223.
Coles, S., 2001. An Introduction to Statistical Modeling of Extreme Values. Springer-Verlag London Limited, Great Britain, pp. 208 pp.
Collins, M.J., 2009. Evidence for changing flood risk in New England since the late 20th Century. J. Am. Water Resour. Assoc. 45 (2), 279–290.

Comte, L., Buisson, L., Daufresne, M., Grenouillet, G., 2013. Climate-induced changes in the distribution of freshwater fish: observed and predicted trends. Freshwater Biol. 58 (4), 625–639.
Daly, C., Neilson, R.P., Phillips, D.L., 1994. A statistical topographic model for mapping climatological precipitation over mountainous terrain. J. Appl. Meteorol. 33 (2), 140–158.
Das, T., Dettinger, M.D., Cayan, D.R., Hidalgo, H.G., 2011. Potential increase in floods in California's Sierra Nevada under future climate projections. Clim. Change 109, 71–94.
Dominguez, F., Canon, J., Valdes, J., 2010. IPCC-AR4 climate simulations for the southwestern US: the importance of future ENSO projections. Clim. Change 99 (3–4), 499–514.
Douglas, E.M., Fairbank, C.A., 2011. Is precipitation in Northern New England becoming more extreme? Statistical analysis of extreme rainfall in Massachusetts, New Hampshire, and Maine and updated estimates of the 100-year storm. J. Hydrol. Eng. 16 (3), 203–217.
Douglas, E.M., Vogel, R.M., Kroll, C.N., 2000. Trends in floods and low flows in the United States: impact of spatial correlation. J. Hydrol. 240 (1–2), 90–105.
Duan, Q.Y., Sorooshian, S., Gupta, V., 1992. Effective and efficient global optimization for conceptual rainfall-runoff models. Water Resour. Res. 28 (4), 1015–1031.
Easterling, D.R., et al., 2000. Climate extremes: observations, modeling, and impacts. Science 289 (5487), 2068–2074.
Falcone, J.D., Carlisle, D.M., Wolock, D.M., Meador, M.R., 2010. GAGES: a stream gage database for evaluating natural and altered flow conditions in the conterminous United States. Ecology 91, 621.
Fan, Y., van den Dool, H., 2008. A global monthly land surface air temperature analysis for 1948-present. J. Geophys. Res.-Atmos. 113 (D1), D01103 1-18.
Fan, F., Bradley, R.S., Rawlins, M.A., 2014. Climate change in the Nrotheastern US: regional climate model validation and climate change projections. Clim. Dyn.
Frei, A., Kunkel, K.E., Matonse, A., 2015. The seasonal nature of extreme hydrological events in the Northeastern United States. J. Hydrometeorol. 16 (5), 2065–2085.
Giorgi, F., Mearns, L.O., 2002. Calculation of average, uncertainty range, and reliability of regional climate changes from AOGCM simulations via the reliability ensemble averaging (REA) method. J. Clim. 15 (10), 1141–1158.
Groisman, P.Y., Knight, R.W., Karl, T.R., 2001. Heavy precipitation and high streamflow in the contiguous United States: trends in the twentieth century. Bull. Am. Meteorol. Soc. 82 (2), 219–246.
Guilbert, J., Betts, A.K., Rizzo, D.M., Beckage, B., Bomblies, A., 2015. Characterization of increased persistence and intensity of precipitation in the northeastern United States. Geophys. Res. Lett. 42 (6), 1888–1893.
Gupta, H.V., Kling, H., Yilmaz, K.K., Martinez, G.F., 2009. Decomposition of the mean squared error and NSE performance criteria: implications for improving hydrological modelling. J. Hydrol. 377 (1–2), 80–91.
Gutmann, E., et al., 2014. An intercomparison of statistical downscaling methods used for water resource assessments in the United States. Water Resour. Res. 50 (9), 7167–7186.
Hayhoe, K., et al., 2007. Past and future changes in climate and hydrological indicators in the US Northeast. Clim. Dyn. 28 (4), 381–407.
Hayhoe, K., et al., 2008. Regional climate change projections for the Northeast USA. Mitig. Adaptation Strategies Global Change 13 (5–6), 425–436.
Helsel, D.R., Hirsch, R.M., 2002. Statistical Methods in Water Resources, Chapter 3, U.S. Geological Survey.
Hodgkins, G.A., Dudley, R.W., 2006. Changes in late-winter snowpack depth, water equivalent, and density in Maine,–2004. Hydrol. Processes 20 (4), 741–751.
Hodgkins, G.A., Dudley, R.W., Huntington, T.G., 2005. Summer low flows in New England during the 20th century. J. Am. Water Resour. Assoc. 41 (2), 403–411.
Hurkmans, R., et al., 2010. Changes in Streamflow dynamics in the rhine basin under three high-resolution regional climate scenarios. J. Clim. 23 (3), 679–699.
Kendall, M.G., 1975. Rank Correlation Methods. Charles Griffin, London.
King, M.C., Mody, N.A., 2010. Numerical and Statistical Methods for Bioengineering. Aplication in MATLAB. Cambridge University Press, New York.
Liang, X., Lettenmaier, D.P., Wood, E.F., Burges, S.J., 1994. A simple hydrologicall based model of land-surface water and energy fluxes for General Circulation Models. J. Geophys. Res.-Atmos. 99 (D7), 14415–14428.
Liang, X., Wood, E.F., Lettenmaier, D.P., 1996. Surface soil moisture parameterization of the VIC-2L model: evaluation and modification. Global Planet. Change 13 (1–4), 195–206.
Liang, X.-Z., et al., 2012. Regional climate-weather research and forecasting model. B. Am. Meteorol. Soc. 93 (9), 1363–1387.
Lins, H.F., Slack, J.R., 1999. Streamflow trends in the United States. Geophys. Res. Lett. 26 (2), 227–230.
Lins, H.F., Slack, J.R., 2005. Seasonal and regional characteristics of US streamflow trends in the United States from 1940 to 1999. Phys. Geogr. 26 (6), 489–501.
Liuzzo, L., Freni, G., 2015. Analysis of extreme rainfall trends in sicily for the evaluation of depth-duration-frequency curves in climate change scenarios. J. Hydrol. Eng. 20 (12), 1943–5584.
Livezey, R.E., Vinnikov, K.Y., Timofeyeva, M.M., Tinker, R., van den Dool, H.M., 2007. Estimation and extrapolation of climate normals and climatic trends. J. Appl. Meteorol. Climatol. 46 (11), 1759–1776.
Lohmann, D., Raschke, E., Nijssen, B., Lettenmaier, D.P., 1998. Regional scale hydrology: I. formulation of the VIC-2L model coupled to a routing model. Hydrol. Sci. J. 43 (1), 131–141.
Mallakpour, I., Villarini, G., 2015. The changing nature of flooding across the central United States. Nat. Clim. Change 5 (3), 250–254.
Mann, H.B., 1945. Nonparametric tests against trend. Econometrica 13 (3), 245–259.
Marshall, E., Randhir, T., 2008. Effect of climate change on watershed system: a regional analysis. Clim. Change 89 (3–4), 263–280.
Maurer, E.P., Wood, A.W., Adam, J.C., Lettenmaier, D.P., Nijssen, B., 2002. A long-term hydrologically based dataset of land surface fluxes and states for the conterminous United States. J. Clim. 15 (22), 3237–3251.
Maurer, E.P., Brekke, L., Pruitt, T., Duffy, P.B., 2007. Fine-resolution climate projections enhance regional climate change impact studies. Eos Trans. AGU 88 (407), 504.
Maurer, E.P., Adam, J.C., Wood, A.W., 2009. Climate model based consensus on the hydrologic impacts of climate change to the Rio Lempa basin of Central America. Hydrol. Earth Syst. Sci. 13 (2), 183–194.
Maurer, E.P., Brekke, L.D., Pruitt, T., 2010a. Contrasting lumped and distributed hydrology models for estimating climate change impacts on california watersheds. J. Am. Water Resour. Assoc. 46 (5), 1024–1035.
Maurer, E.P., Hidalgo, H.G., Das, T., Dettinger, M.D., Cayan, D.R., 2010b. The utility of daily large-scale climate data in the assessment of climate change impacts on daily streamflow in California. Hydrol. Earth Syst. Sci. 14 (6), 1125–1138.
McCabe, G.J., Wolock, D.M., 2002. A step increase in streamflow in the conterminous United States. Geophys. Res. Lett. 29 (24), W11522 1-11.
McCabe, G.J., Wolock, D.M., 2011. Independent effects of temperature and precipitation on modeled runoff in the conterminous United States. Water Resour. Res. 47, W11522 1-11.
Mishra, V., Lettenmaier, D.P., 2011. Climatic trends in major US urban areas, 1950–2009. Geophys. Res. Lett., 38.
Moriasi, D.N., et al., 2007. Model evaluation guidelines for systematic quantification of accuracy in watershed simulations. Trans. Asabe 50 (3), 885–900.
NRCS, 2004. National Engineering Handbook: Estimation of Direct Runoff from Storm Rainfall. USDA-NRCS.
Nag, B., Misra, V., Bastola, S., 2014. Validating ENSO teleconnections on southeastern US winter hydrology. Earth Interact., 18.
Namias, J., 1966. Nature and possible causes of northeastern United States drought during 1962–65. Mon. Weather Rev. 94 (9), 543-&.
New, M., Lister, D., Hulme, M., Makin, I., 2002. A high-resolution data set of surface climate over global land areas. Clim. Res 21 (1), 1–25.

Ning, L., Bradley, R.S., 2014. Winter precipitation variability and corresponding teleconnections over the northeastern United States. J. Geophys. Res.-Atmos. 119 (13), 7931–7945.
Panofsky, H.A., Brier, G.W., 1968. Some Applications of Statistics to Meteorology. The Pennsylvania State University, University Park, PA, USA, pp. 224 pp.
Pettitt, A.N., 1979. A non-parametric approach to the change-point problem. Appl. Stat. 28 (2), 126–135.
Rawlins, M.A., Bradley, R.S., Diaz, H.F., 2012. Assessment of regional climate model simulation estimates over the northeast United States. J. Geophys. Res.-Atmos. 117, D23112 1-15.
Risley, J., Stonewall, A., Haluska, T., 2008. Estimating Flow-Duration and Low-Flow Frequency Statistics for Unregulated Streams in Oregon, U.S. Geological Survey.
Sawaske, S.R., Freyberg, D.L., 2014. An analysis of trends in baseflow recession and low-flows in rain-dominated coastal streams of the pacific coast. J. Hydrol. 519, 599–610.
Sen, P.K., 1968. Estimates of the regression coefficient based on Kendall's tau. J. Am. Stat. Assoc. 63 (324), 1379–1389.
Serinaldi, F., Kilsby, C.G., 2015. The importance of prewhitening in change point analysis under persistence. Stochastic Environ. Res. Risk Assess., 1–15.
Small, D., Islam, S., Vogel, R.M., 2006. Trends in precipitation and streamflow in the eastern US: paradox or perception? Geophys. Res. Lett. 33 (3), L03403.
Taylor, K.E., Stouffer, R.J., Meehl, G.A., 2012. An Overview of CMIP5 and the experiment design. Bull. Am. Met. Soc. 93, 485–498, http://dx.doi.org/10.1175/bams-d-11-00094.1.
Tebaldi, C., Knutti, R., 2007. The use of the multi-model ensemble in probabilistic climate projections. Philos. Trans. R. Soc. A 365 (1857), 2053–2075.
Themessl, M.J., Gobiet, A., Leuprecht, A., 2011. Empirical-statistical downscaling and error correction of daily precipitation from regional climate models. Int. J. Climatol. 31 (10), 1530–1544.
Thibeault, J.M., Seth, A., 2014. Changing climate extremes in the Northeast United States: observations and projections from CMIP5. Clim. Change 127 (2), 273–287.
Trenberth, K.E., Dai, A., Rasmussen, R.M., Parsons, D.B., 2003. The changing character of precipitation. B. Am. Meteorol. Soc. 84 (9), 1205–1217.
Troy, T.J., Wood, E.F., Sheffield, J., 2008. An efficient calibration method for continental-scale land surface modeling. Water Resour. Res. 44 (9).
Vano, J.A., et al., 2014. Understanding uncertainties in future Colorado river streamflow. B. Am. Meteorol. Soc. 95 (1), 59–78.
Vicente-Serrano, S.M., et al., 2012. Accurate computation of a streamflow drought index. J. Hydrol. Eng. 17 (2), 318–332.
Villarini, G., Smith, J.A., 2010. Flood peak distributions for the eastern United States. Water Resour. Res. 46.
Villarini, G., Smith, J.A., Baeck, M.L., Krajewski, W.F., 2011. Examining Flood frequency distributions in the midwest U. S. J. Am. Water Resour. Assoc. 47 (3), 447–463.
WMO, 2009. Manual on Low-flow Estimation and Predictions. WMO, Geneva, Switzerland.
Walsh, J., et al., 2014. Our changing climate. In: Climate Change Impacts in the United States, U. S. Global Change Research Program USA.
Wilks, D.S., 2006. Statistical Methods in the Atmospheric Sciences, 2nd ed. Academic Press, New York, NY, USA, pp. 627 pp.
Wood, A.W., Maurer, E.P., Kumar, A., Lettenmaier, D.P., 2002. Long-range experimental hydrologic forecasting for the eastern United States. J. Geophys. Res.-Atmos. 107 (D20).
Wood, A.W., Leung, L.R., Sridhar, V., Lettenmaier, D.P., 2004. Hydrologic implications of dynamical and statistical approaches to downscaling climate model outputs. Clim. Change 62 (1–3), 189–216.
Xia, Y., et al., 2012. Continental-scale water and energy flux analysis and validation for the North American Land data assimilation system project phase 2 (NLDAS-2): 1. Intercomparison and application of model products. J. Geophys. Res.-Atmos. 117, D03109.
Yilmaz, K.K., Gupta, H.V., Wagener, T., 2008. A process-based diagnostic approach to model evaluation: Application to the NWS distributed hydrologic model. Water Resour. Res. 44 (9).
Yuan, X., Wood, E.F., Roundy, J.K., Pan, M., 2013. CFSv2-based seasonal hydroclimatic forecasts over the conterminous United States. J. Clim. 26 (13), 4828–4847.
Yue, S., Pilon, P., Phinney, B., Cavadias, G., 2002. The influence of autocorrelation on the ability to detect trend in hydrological series. Hydrol. Processes 16 (9), 1807–1829.